

Prognostic relevance of clonal hematopoiesis in myeloid neoplastic transformation in patients with follicular lymphoma treated with radioimmunotherapy

Zhuoer Xie,^{1,2} Terra Lasho,¹ Arushi Khurana,¹ Alejandro Ferrer,¹ Christy Finke,¹ Abhishek A. Mangaonkar,¹ Stephen Ansell,¹ Jenna Fernandez,¹ Mithun Vinod Shah,¹ Aref Al-Kali,¹ Naseema Gangat,¹ Jithma Abeykoon,¹ Thomas E. Witzig¹ and Mrinal M. Patnaik¹

¹Mayo Clinic, Department of Internal Medicine, Hematology Division, Rochester, MN and

²Malignant Hematology Department, H. Lee Moffitt Cancer Center & Research Institute, Tampa, FL, USA

Correspondence: M. Patnaik
Patnaik.Mrinal@mayo.edu

Received: June 13, 2023.

Accepted: August 16, 2023.

Early view: August 31, 2023.

<https://doi.org/10.3324/haematol.2023.283727>

©2024 Ferrata Storti Foundation

Published under a CC BY-NC license



Supplemental information.

DNA sequencing method: briefly 200 ng of target DNA was fragmented using the Covaris LE220 plus sonicator. The ends were repaired using the Sureselect End-Repair-A-Tailing enzyme mix. Adapter ligated DNA fragments were size selected to enrich for 200 bp inserts (~320 bp total library size) using AMPURE XP bead purification. The size selected adapter-modified fragments were enriched, and specific indexes were added by 12 cycles of PCR using universal Index Primers.

The Custom Capture hybrid-target enrichment probes were designed using Agilent SureSelect design software (Agilent Technologies, Santa Clara, CA). The targeted gene panel was comprised of 62962 single probes with size 1.805Mbp, and covered the coding regions, UTRs, and overlapping intron/exon regions for 205 genes described and/or enriched for CHIP mutations. The custom capture was carried out using the Agilent Bravo liquid handler following Agilent's SureSelect XT Low. Purified capture products were then amplified using the SureSelect Post-Capture primer mix for 14 cycles. Libraries were validated and quantified on the Agilent Bioanalyzer. Samples were sequenced by 150 paired end reads, 21 samples to a Flow Cell, on an Illumina NovaSeqSP with an expected depth of $\geq 1,000X$ coverage (Illumina, SanDiego, CA).

Secondary bioinformatics analysis included quality assessment and alignment to the hg19 build reference genome using Novoalign (Novo-craft Technologies, Malaysia), followed by GATK based single nucleotide and small insertion/deletion variant calling, structural variation discovery, and annotation. The quality of sequencing chemistry was evaluated using FastQC ('FASTQC'). After alignment, PCR duplication rates and percent reads mapped on target were used to assess the quality of the sample preps. Realignment and recalibration steps were implemented in the GATK. Somatic single nucleotide variations (SNVs) were then genotyped using SomaticSniper, whereas insertions and deletions were called by GATK Somatic Indel Detector. Each variant in coding regions was Strand-Aware Variant Annotation Tool '), as well as ClinVar, dbNSFP, OMIM, and the Human Gene Annotation Database to predict biological effects. Interpretation for relevant alterations included absence in international normal variant allele databases (GnomAD, ExAC), deleterious effect on protein function by multiple phenotype prediction models, somatic and functional annotation in literature, consequence of variant (nonsense, truncating, etc.) and location proximal to important domains.

Supplementary Table 1. The CH panel used in the study covered 289 genes.

ANKRD26
ARID1A
ASXL1
ASXL2
ATM
BCL10
BCL11B
BCL6
BCOR
BCORL1
BIRC3
BRAF
BRCC3
BTG1
BTG2
CALR
CARD11
CBL
CBLB
CCND3
CD58
CD70
CD79A
CD79B
CDKN2A
CDKN2B
CEBPA
CHD2
CNOT3
CREBBP
CRLF2
CSF1R
CHEK2
CSF3R
CTCF
CUX1
DDX3X
DDX41
DIS3
DNMT3A
DNMT3B
EBF1
EED
EP300
ETNK1
ETV6
EZH2
ELANE
ERCC6L2
EZR
FAM46C
FAS
FBXO11
FBXW7
FLT3
FOXP1
FYN
GATA1
GATA2
GATA3
GNA13
GNAS
GNB1
HIST1H1B
HIST1H1C
HIST1H1D
HIST1H1E
HIST1H3B
HRAS
ID3
IDH1
IDH2
IDH3A
IKBKB
IKZF1
IKZF2
IKZF3
IL7R
INTS12
IRF4
IRF8

ITK
JAK1
JAK2
JAK3
JARID2
KDM6A
KDM5A
KDM5C
KIT
KLHL6
KMT2A
KMT2B
KMT2C
KMT2D
KRAS
LEF1
LRBA
LRRK2
LTB
LUC7L2
MALT1
MAP2K1
MAP3K14
MAPK1
MED12
MEF2B
MPL
MXRA5
MYD88
MECOM
NF1
NOTCH1
NOTCH2
NPM1
NRAS
P2RY8
PAPD5
PAX5
PDS5B
PDSS2
PHF6
PHIP
PIK3CA
PML
POT1
POU2AF1
POU2F2
PPM1D
PRDM1
PRPF40B
PRPF8
PTEN
PTPN1
PTPN11
RAD21
RBBP4
RHOA
RIT1
RPL10
RPL5
RPS15
RPS2
RUNX1
SETBP1
SETD2
SETDB1
SF1
SF3A1
SF3B1
SGK1
SMC1A
SMC3
SOCS1
SPRY4
SRSF2
STAG1
STAG2
STAT3
STAT5A
STAT5B
STAT6
STK11
STK35
SUZ12

SWAP70
TBL1XR1
TCF3
TET1
TET2
TET3
TMEM30A
TNF
TNFAIP3
TNFRSF14
TP53
TRAF3
TYW1
U2AF1
U2AF2
UBR5
VPS13B
VPS13C
VWF
WT1
XBP1
XPO1
ZNF471
ZRSR2

Supplementary table 2. The pathogenic variants identified in the entire cohort.

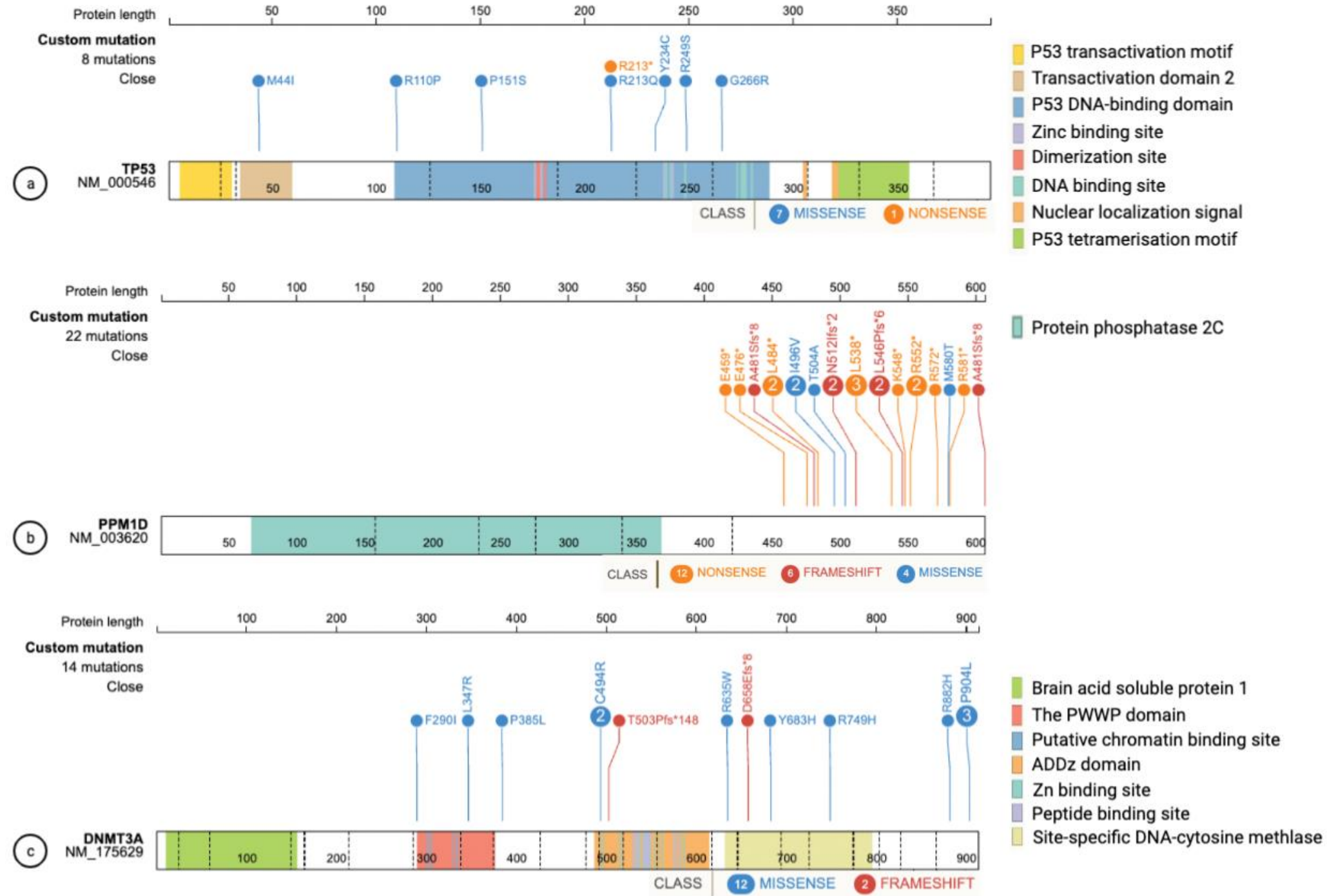
| | Gene | Chromosome | Nucleotide change | Amino acid change | Mutation type | CH type |
|-------|-----------------|------------|----------------------------|-------------------|---------------|---------|
| PT_17 | <i>JAK2</i> | 9 | c.1711G>A | G571S | Missense | M-CH |
| | <i>PPM1D</i> | 17 | c.1654C>T | R552* | Nonsense | |
| | <i>TP53</i> | 17 | c.329G>C | R110P | Missense | |
| PT_18 | <i>ASXL1</i> | 20 | c.4342C>T | Q1448* | Nonsense | LM-CH |
| | <i>NOTCH1</i> | 9 | c.1295C>T | T432M | Missense | |
| | <i>PPM1D</i> | 17 | c.1375G>T | E459* | Nonsense | |
| | <i>PPM1D</i> | 17 | c.1613T>G | L538* | Nonsense | |
| | <i>SMC3</i> | 10 | c.2000G>T | G667V | Missense | |
| PT_19 | <i>PPM1D</i> | 17 | c.1535delA | N512Ifs*2 | Frameshift | M-CH |
| | <i>TP53</i> | 17 | c.701A>G | Y234C | Missense | |
| PT_20 | <i>CBL</i> | 11 | c.1247G>T | C416F | Missense | LM-CH |
| | <i>CREBBP</i> | 16 | c.1909G>T | E637* | Missense | |
| | <i>KMT2D</i> | 12 | c.11584C>T | Q3862* | Nonsense | |
| | <i>LTB</i> | 6 | c.199C>A | Q67K | Missense | |
| | <i>STAT6</i> | 12 | c.1256A>G | D419G | Missense | |
| PT_21 | <i>PPM1D</i> | 17 | c.1642A>T | K548* | Nonsense | M-CH |
| PT_22 | <i>EZH2</i> | 7 | c.338G>A | W113* | Nonsense | LM-CH |
| | <i>IDH2</i> | 15 | c.515G>A | R172K | Missense | |
| | <i>PPM1D</i> | 17 | c.1440dupA | A481Sfs*8 | Frameshift | |
| | <i>STAG2</i> | X | c.1664_1667dupCACA | Q556Hfs*5 | Frameshift | |
| PT_23 | <i>KMT2D</i> | 12 | c.8704C>T | Q2902* | Nonsense | L-CH |
| PT_24 | <i>DNMT3A</i> | 2 | c.1974_1978del | D658Efs*8 | Frameshift | M-CH |
| PT_25 | <i>DNMT3A</i> | 2 | c.1480T>C | C494R | Missense | LM-CH |
| | <i>KMT2D</i> | 12 | c.11905C>T | Q3969* | Nonsense | |
| | <i>KMT2D</i> | 12 | c.8488C>T | R2830* | Nonsense | |
| PT_26 | <i>CDKN2A</i> | 9 | c.238C>T | R80* | Nonsense | LM-CH |
| | <i>CREBBP</i> | 16 | c.4336C>T | R1446C | Missense | |
| | <i>DNMT3A</i> | 2 | c.2711C>T | P904L | Missense | |
| | <i>PPM1D</i> | 17 | c.1741C>T | R581* | Nonsense | |
| | <i>PPM1D</i> | 17 | c.1654C>T | R552* | Nonsense | |
| | <i>PPM1D</i> | 17 | c.1714C>T | R572* | Nonsense | |
| PT_27 | <i>HIST1H1C</i> | 6 | c.280G>A | V94M | Missense | LM-CH |
| | <i>PPM1D</i> | 17 | c.1486A>G | I496V | Missense | |
| | <i>PPM1D</i> | 17 | c.1636dupC | L546Pfs*6 | Frameshift | |
| PT_28 | <i>PPM1D</i> | 17 | L538* | L538* | Nonsense | M-CH |
| | <i>PPM1D</i> | 17 | A481Sfs*8 | A481Sfs*8 | Frameshift | |
| | <i>TET2</i> | 4 | c.3804-2A>G | splice effect | Splice Effect | |
| PT_29 | <i>ASXL1</i> | 20 | c.1782C>A | C594* | Nonsense | M-CH |
| | <i>TP53</i> | 17 | c.747G>T | R249S | Missense | |
| PT_30 | <i>ARID1B</i> | 6 | c.662del | N221Tfs*42 | Frameshift | LM-CH |
| | <i>DNMT3A</i> | 2 | c.1506del | T503Pfs*148 | Frameshift | |
| | <i>MED12</i> | X | c.6348_6359dupCCAGCAGCAACA | H2116_Q2119dup | Duplication | |
| | <i>STAT3</i> | 17 | c.1973A>G | K658R | Missense | |
| PT_31 | <i>DNMT3A</i> | 2 | c.1040T>G | L347R | Missense | M-CH |
| | <i>DNMT3A</i> | 2 | c.2173+1G>A | splice effect | Splice Effect | |
| PT_32 | <i>BRCC3</i> | X | c.721C>T | Q241* | Nonsense | M-CH |
| | <i>PPM1D</i> | 17 | c.1613T>G | L538* | Nonsense | |
| PT_33 | <i>ASXL2</i> | 2 | c.3715G>T | E1239* | Nonsense | LM-CH |
| | <i>CARD11</i> | 7 | c.583G>C | V195L | Missense | |
| | <i>DNMT3A</i> | 2 | c.2173+1G>A | splice effect | Splice Effect | |
| | <i>DNMT3A</i> | 2 | c.2645G>A | R882H | Missense | |
| | <i>DNMT3A</i> | 2 | c.2083-2A>G | splice effect | Splice Effect | |
| | <i>EP300</i> | 22 | c.784G>T | G262* | Nonsense | |
| | <i>PHIP</i> | 6 | c.2785G>T | E929* | Nonsense | |
| | <i>PPM1D</i> | 17 | c.1510A>G | T504A | Missense | |
| | <i>PPM1D</i> | 17 | c.1451T>A | L484* | Nonsense | |
| | <i>TET1</i> | 10 | c.2077G>T | E693* | Nonsense | |
| PT_34 | <i>JAK2</i> | 9 | c.365G>A | R122H | Missense | LM-CH |
| | <i>STAT6</i> | 12 | c.3G>A | p.Met1? | Nonsense | |
| PT_35 | <i>DNMT3A</i> | 2 | c.2711C>T | P904L | Missense | M-CH |
| | <i>TP53</i> | 17 | c.451C>T | P151S | Missense | |
| PT_36 | <i>DNMT3A</i> | 2 | c.1903C>T | R635W | Missense | M-CH |
| PT_37 | <i>DNMT3A</i> | 2 | c.2711C>T | P904L | Missense | M-CH |
| | <i>DNMT3A</i> | 2 | c.868T>A | F290I | Missense | |
| PT_38 | <i>DNMT3A</i> | 2 | c.1A>C | p.Met1? | Nonsense | M-CH |
| | <i>DNMT3A</i> | 2 | c.2246G>A | R749H | Missense | |
| | <i>PPM1D</i> | 17 | c.1636dupC | L546Pfs*6 | Frameshift | |

| | | | | | | |
|-------|-----------------|----|----------------------------|----------------|---------------|-------|
| | <i>PPM1D</i> | 17 | c.1535delA | N512Ifs*2 | Frameshift | |
| PT_39 | <i>PPM1D</i> | 17 | c.1451T>G | L484* | Nonsense | M-CH |
| PT_40 | <i>PPM1D</i> | 17 | c.1739T>C | M580T | Missense | M-CH |
| | <i>SBDS</i> | 7 | c.127G>T | V43L | Missense | |
| | <i>TP53</i> | 17 | c.638G>A | R213Q | Missense | |
| | <i>TP53</i> | 17 | c.796G>A | G266R | Missense | |
| PT_41 | <i>DNMT3A</i> | 2 | c.1154C>T | P385L | Missense | M-CH |
| PT_42 | <i>DNMT3A</i> | 2 | c.2047T>C | Y683H | Missense | M-CH |
| PT_43 | <i>ARID1A</i> | 1 | c.3036T>G | Y1012* | Nonsense | LM-CH |
| | <i>CREBBP</i> | 16 | c.4297_4305del | Y1433_D1435del | Deletion | |
| | <i>KMT2D</i> | 12 | c.5104C>T | R1702* | Nonsense | |
| | <i>NF1</i> | 17 | c.3826C>T | R1276* | Nonsense | |
| PT_44 | <i>DNMT3A</i> | 2 | c.2173+1G>A | splice effect | Splice Effect | M-CH |
| PT_45 | <i>MED12</i> | X | c.6348_6359dupCCAGCAGCAACA | H2116_Q2119dup | Duplication | M-CH |
| PT_53 | <i>CD79B</i> | 17 | c.586T>G | Y197D | Missense | LM-CH |
| | <i>CREBBP</i> | 16 | c.4336C>T | R1446C | Missense | |
| | <i>HIST1H1C</i> | 6 | c.305C>T | S102F | Missense | |
| | <i>KMT2D</i> | 12 | c.15289C>T | R5097* | Nonsense | |
| | <i>TP53</i> | 17 | c.637C>T | R213* | Nonsense | |
| PT_54 | <i>PHIP</i> | 6 | c.607G>T | D203Y | Missense | M-CH |
| | <i>PPM1D</i> | 17 | c.1426G>T | E476* | Nonsense | |
| | <i>TP53</i> | 17 | c.132G>T | M44I | Missense | |
| | <i>DNMT3A</i> | 2 | c.1480T>C | C494R | Missense | |
| PT_55 | <i>PTEN</i> | 10 | c.253+42C>T | splice effect | Splice Effect | M-CH |
| PT_56 | <i>EZH2</i> | 7 | c.1852-6C>T | splice effect | Splice Effect | L-CH |
| PT_57 | <i>PPM1D</i> | 17 | c.1486A>G | I496V | Missense | M-CH |
| PT_58 | <i>CREBBP</i> | 16 | c.4424C>T | P1475L | Missense | LM-CH |
| | <i>EZH2</i> | 7 | c.1937A>C | Y646S | Missense | |
| | <i>KMT2D</i> | 12 | c.13745_13764del | G4582Efs*17 | Frameshift | |
| | <i>KMT2D</i> | 12 | c.14515+2T>G | splice effect | Splice Effect | |
| | <i>POU2AF1</i> | 11 | c.16+3A>T | splice effect | Splice Effect | |
| | <i>TNFRSF14</i> | 1 | c.169T>C | C57R | Missense | |

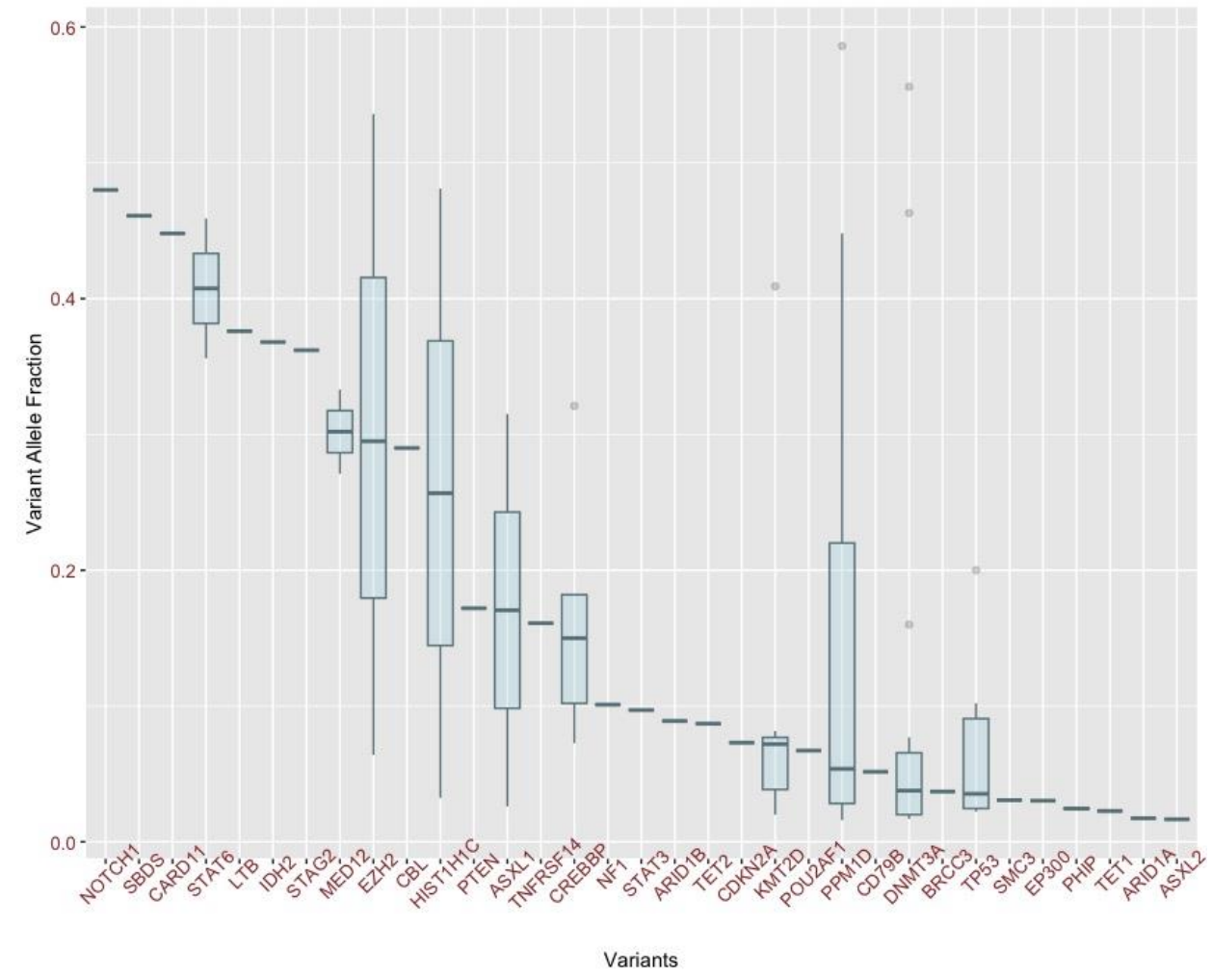
Supplementary Table 3. Detailed information for group 1, including the time differences between the paired samples.

| | Age | Gender | Total number of mutations | Type of Mutation | Time to Zevalin (y) | Timing diff for the paired sample (y) | TMN | Zevalin To TMN | Zevalin to Last FU | Death | OS |
|-------|-----|--------|---------------------------|------------------|---------------------|---------------------------------------|-----|----------------|--------------------|-------|-------|
| PT_9 | 79 | M | 0 | - | 1.86 | 1.01 | Y | 9.60 | 10.00 | Y | 11.86 |
| PT_10 | 38 | F | 0 | - | 0.83 | 0.24 | N | | 6.91 | N | 7.74 |
| PT_11 | 36 | M | 0 | - | 0.43 | 1.03 | N | | 15.55 | N | 15.98 |
| PT_12 | 43 | M | 0 | - | 2.27 | 0.72 | N | | 14.45 | N | 16.73 |
| PT_13 | 60 | F | 0 | - | 2.81 | 4.93 | N | | 13.10 | N | 15.91 |
| PT_14 | 42 | F | 0 | - | 7.30 | 1.14 | N | | 10.82 | Y | 18.12 |
| PT_15 | 55 | M | 0 | - | 3.38 | 1.05 | N | | 15.65 | N | 19.03 |
| PT_16 | 63 | F | 0 | - | 9.13 | 1.05 | N | | 15.27 | N | 24.40 |
| PT_30 | 40 | F | 4 | LM-CH | 12.73 | 0.27 | Y | 6.60 | 14.32 | N | 27.05 |
| PT_31 | 50 | M | 2 | M-CH | 8.41 | 1.05 | Y | 7.88 | 7.90 | N | 16.30 |
| PT_32 | 67 | F | 2 | M-CH | 4.11 | 0.93 | Y | 9.81 | 12.01 | Y | 16.12 |
| PT_33 | 45 | M | 10 | LM-CH | 1.30 | 5.20 | N | | 16.98 | N | 18.28 |
| PT_34 | 43 | F | 1 | L-CH | 7.12 | 1.13 | N | | 16.80 | N | 23.92 |
| PT_35 | 36 | F | 2 | M-CH | 32.42 | 1.02 | N | | 5.39 | N | 37.82 |
| PT_36 | 46 | M | 1 | M-CH | 19.64 | 1.01 | N | | 16.21 | N | 35.85 |
| PT_37 | 48 | F | 2 | M-CH | 10.16 | 1.17 | N | | 16.63 | N | 26.79 |
| PT_38 | 69 | M | 4 | M-CH | 4.99 | 0.52 | N | | 16.93 | N | 21.92 |
| PT_39 | 67 | M | 1 | M-CH | 5.02 | 1.07 | N | | 14.85 | Y | 19.87 |
| PT_40 | 70 | F | 4 | M-CH | 3.61 | 0.52 | N | | 12.21 | Y | 15.82 |
| PT_41 | 65 | M | 1 | M-CH | 3.40 | 0.99 | N | | 16.50 | N | 19.90 |
| PT_42 | 66 | F | 1 | M-CH | 10.35 | 1.01 | N | | 7.18 | Y | 17.53 |
| PT_43 | 36 | F | 4 | LM-CH | 1.04 | 1.48 | N | | 18.37 | N | 19.41 |
| PT_44 | 49 | F | 1 | M-CH | 2.46 | 0.80 | N | | 14.65 | N | 17.11 |
| PT_45 | 28 | F | 1 | M-CH | 14.03 | 0.50 | N | | 14.73 | N | 28.76 |

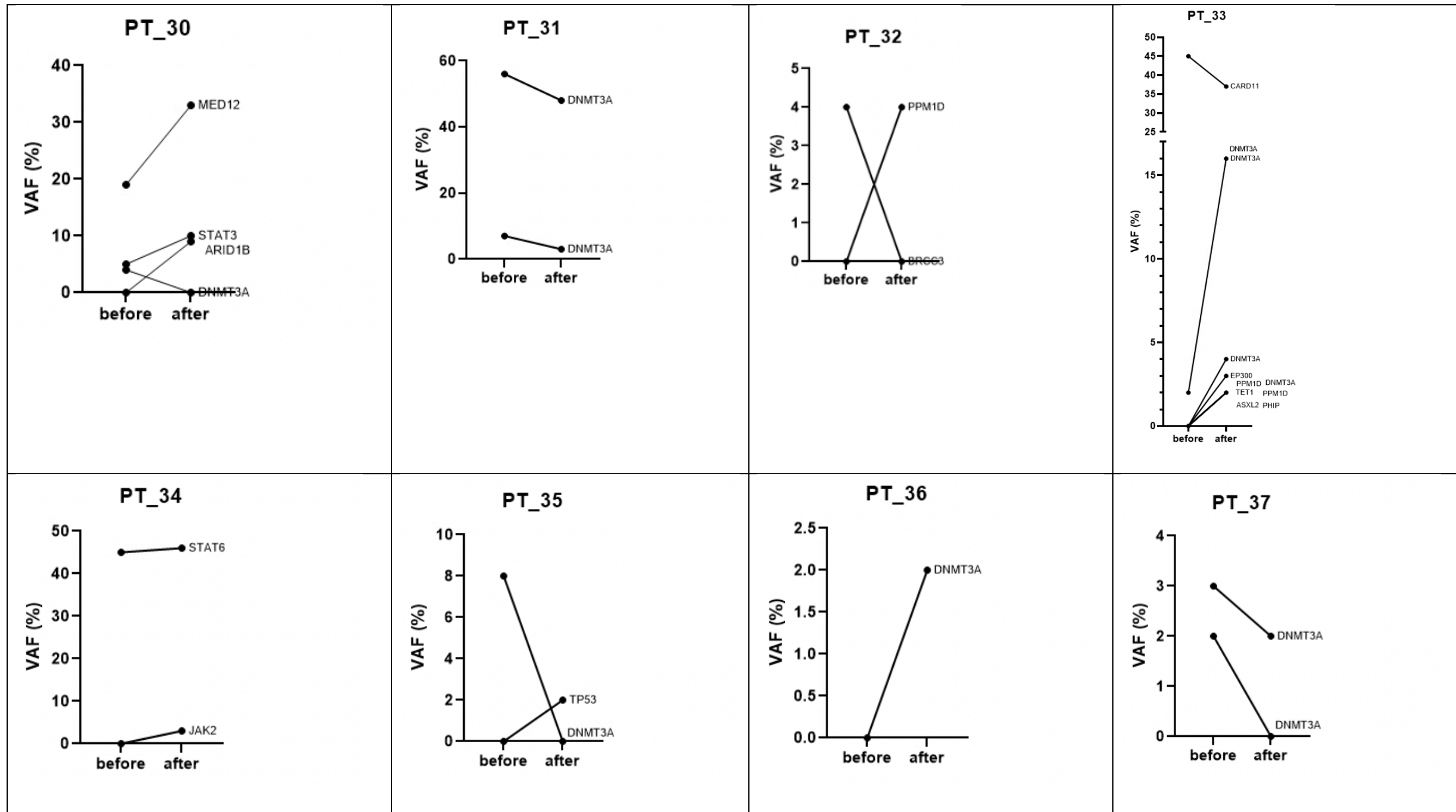
Supplementary Figure 1. Lollipop plot showing type and location along the protein sequence of *TP53* mutation, *PPM1D* mutation, and *DNMT3A* mutation. The number of recurrently detected alterations is indicated by the text within each disc, as well as by disc size. Colors indicate the type of mutation: blue, missense; orange, nonsense; red, frameshift. Most of the *TP53* mutations were missense mutations and occurred in the DNA binding domain, while 82% of the *PPM1D* mutations were truncating mutations that occurred in the terminal exon. *DNMT3A* mutations were largely missense mutations and occurred throughout the genome, with 6 involving the catalytic methyltransferase domain, including 1 dominant negative R882 mutation that has been implicated commonly in MDS/AML

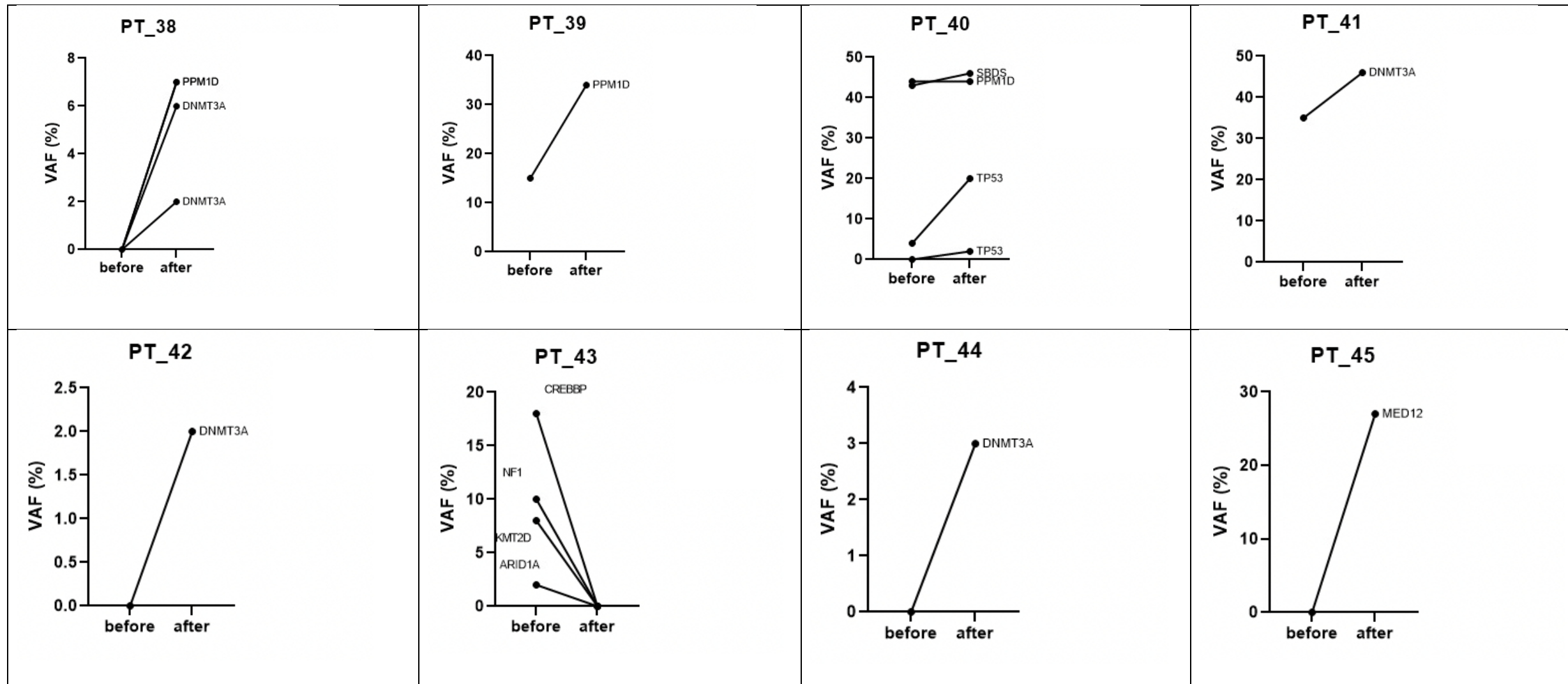


Supplemental figure 2. Variant allele fraction is sorted from the highest to the lowest.

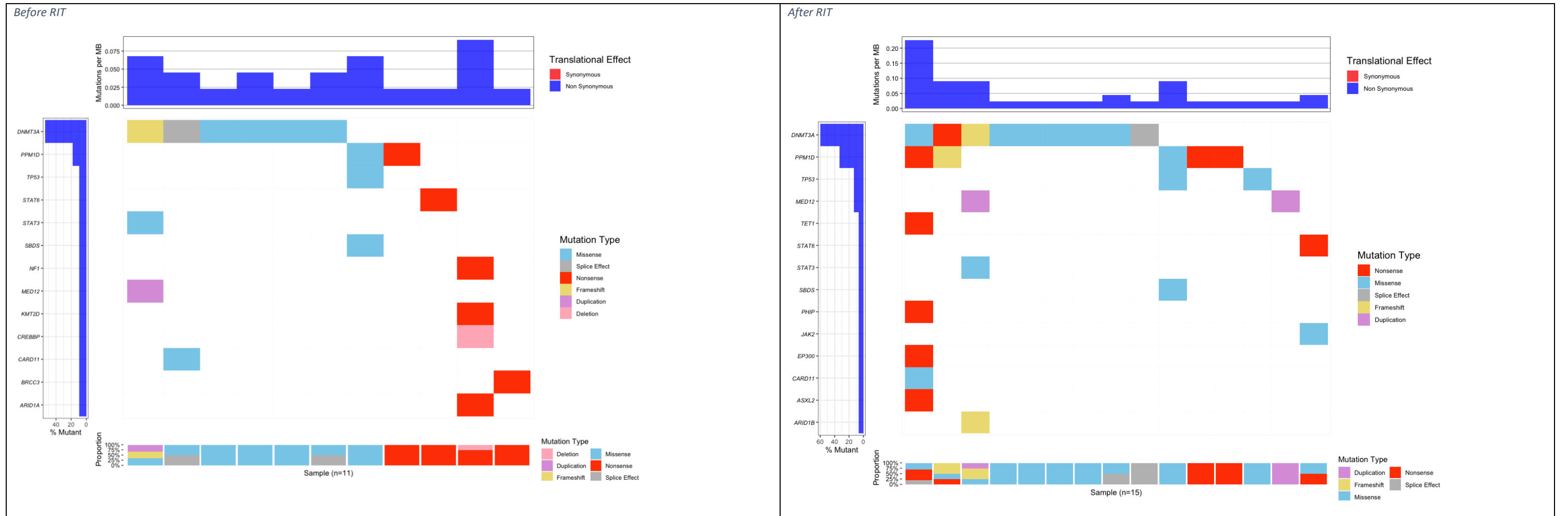


Supplemental figure 3. Clone evolution before and after radioisotope therapy in group 1.

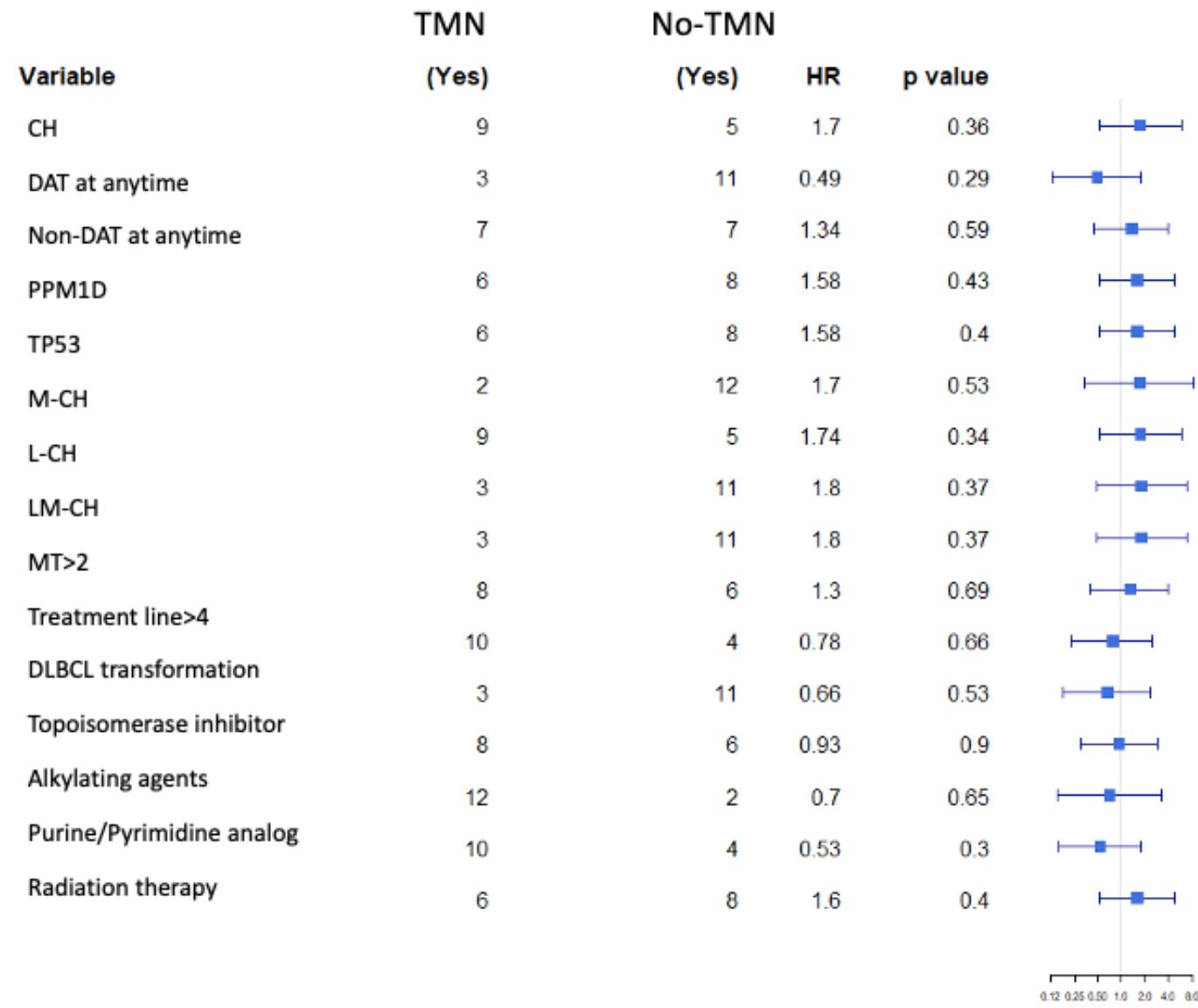




Supplementary Figure 4. Oncoplot before and after radioisotope therapy in group 1.

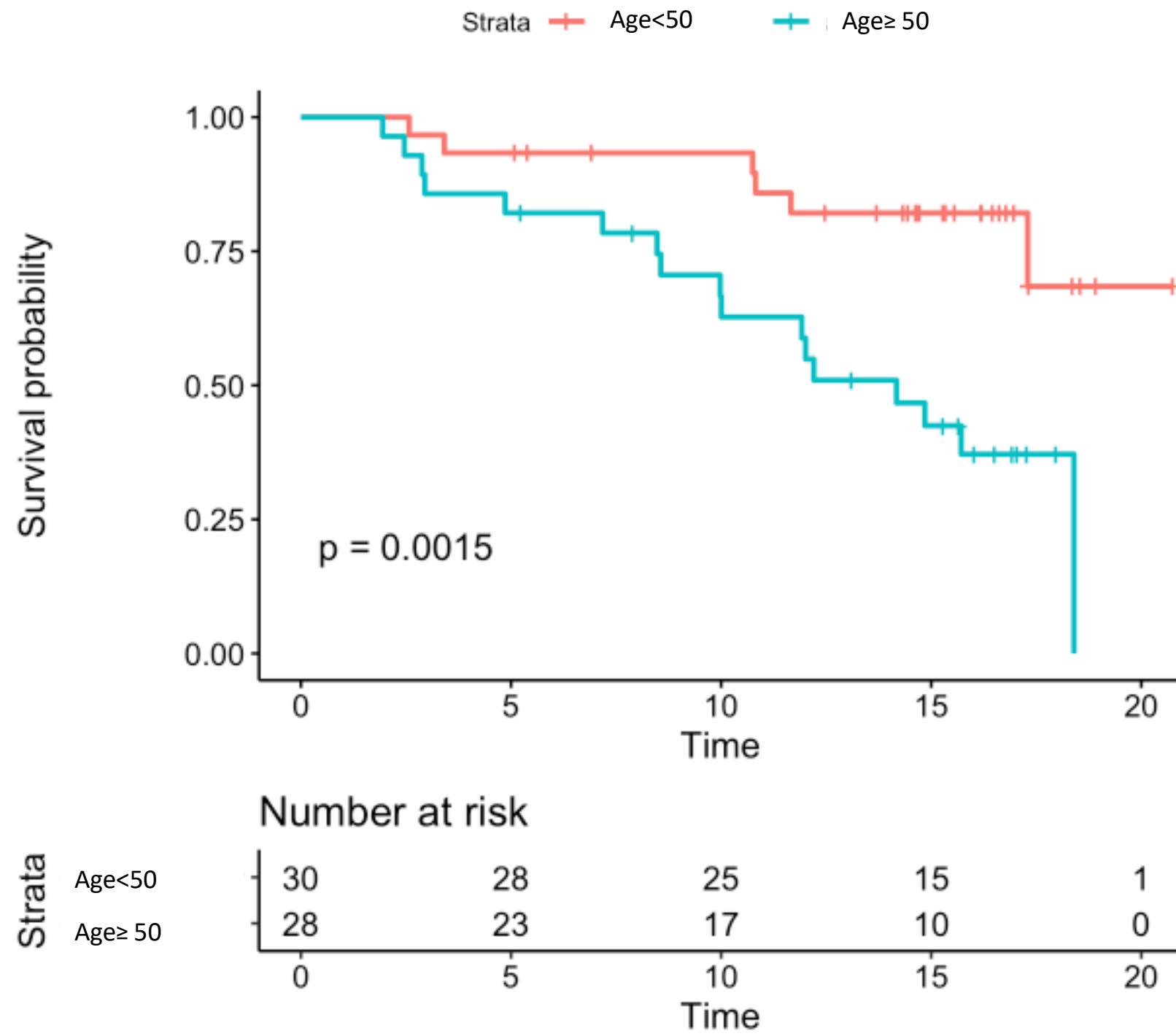


Supplementary Figure 5. Forest plot for the variables on TMN development (univariable analysis);

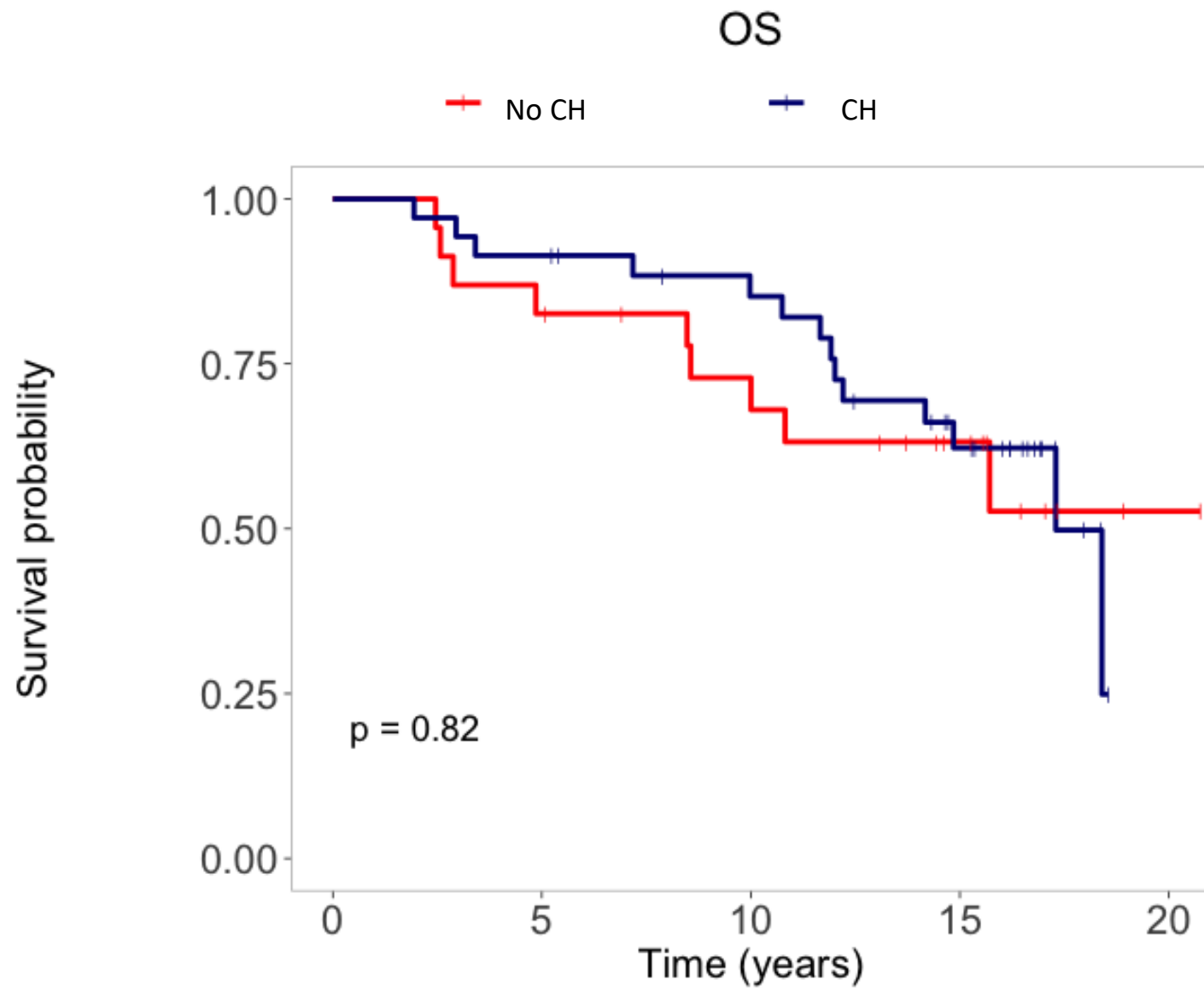


Abbreviation: DAT: *DNMT3A*, *ASXL1*, and *TET2*; AnytimeDAT: DAT mutations at any time points. AnytimeNonDAT: mutations other than DAT mutations at any time points. DDR: DNA damage response and repair; M-CH: myeloid CH; L-CH: lymphoid CH; LM-CH: lymphoid and myeloid CHIP; MT>2: more than 2 mutations.

Supplementary Figure 6. Age>50 is a risk factor for shorter OS. Group 0 indicates age<50, group 1 indicates age ≥ 50



Supplementary Figure 7. Overall survival stratified by CH status.



Number at risk

| | | | | | |
|-------|----|----|----|----|---|
| No CH | 23 | 19 | 15 | 9 | 1 |
| CH | 35 | 32 | 27 | 16 | 0 |